Article

Ground-Runoff Harvesting to Increase Water Availability in Isolated Households on Hilly Mediterranean Islands: A Case Study in a Micro-Catchment of Ibiza (Spain)

Daniele Pedretti [1,*](ID), Inés Roig Palomeque [2] and Stefan Meier [3]

1   Dipartimento di Scienze della Terra 'Ardito Desio', Università degli Studi di Milano, 20133 Milan, Italy
2   Alianza por el Agua de Ibiza y Formentera, 07800 Eivissa, Spain; inesroigpa@gmail.com
3   Naturaleza y Arte, 07830 Sant Josep de Sa Talaia, Spain; naturalezayarte@gmail.com
*   Correspondence: daniele.pedretti@unimi.it

Abstract: Mediterranean islands suffer from a lack of freshwater due to persistent and recursive droughts, limited groundwater availability and mass tourism. In Ibiza (Spain), private estates disconnected from the water distribution network consume about 21% of the total freshwater demand on the island. We conducted a study to evaluate the potential of ground-runoff harvesting (GRH) as a sustainable and inexpensive solution to increase freshwater availability in isolated households in Ibiza. The study involved an innovative modular tank of 40 m^3 buried in the garden of a private property. The tank intercepted runoff forming in a 12,300 m^2 hilly micro-catchment. We found that an extreme rainfall event with an intensity of 65 mm/h was able to create sufficient runoff to fill up the tank in one hour. A curve-number-based rainfall-runoff model was used to simulate the experimental results and to obtain a first-cut estimation of the potential of GRH at the scale of the island. The analysis indicates that, if installed in all forest areas in Ibiza with a similar slope to the study area, a volume of 1.31×10^6 m^3 of freshwater could be harvested per year on the island just from extreme precipitation events. Such a volume of water is equivalent to about 5% of the island's total freshwater budget. The study concludes that GRH is a highly valuable, yet still unexploited opportunity to save large freshwater volumes in dry-climate areas like Ibiza. GRH should be promoted across Mediterranean islands, and it can be easily incorporated within local water regulations.

Keywords: surface runoff; rainwater harvesting; extreme hydroclimatic events; water reuse; Balearic Islands

1. Introduction

In the Mediterranean islands, freshwater is scarce, and its conservation is vital. As surface water bodies are mostly ephemeral streams and intermittent rivers [1], groundwater has, for a long time, been the most important water resource on the islands. Water wells have been used for decades to satisfy the needs of local populations, but with the advent of mass tourism and industry, groundwater has become insufficient to cope with the freshwater demand. Although geological reservoirs on the islands can have large storage capacities and high transmissivities, such as karst aquifers [2,3], their replenishment rate is largely exceeded by well pumping rates. As in continental coastal aquifers [4], this has led to detrimental qualitative (seawater upconing) and quantitative (low groundwater levels) aquifer conditions [5].

During the peak tourism seasons, the floating population in Mediterranean islands grows significantly. For instance, the number of individuals (in.) officially registered on Spain's Balearic Islands grew from a minimum of 1,110,180 in. in December 2016 to 2,057,244 in. in August 2017 (https://www.diariodemallorca.es/mallorca/2017/04/06/balears-supera-primera-vez-millones-3432398.html, [in Spanish]; accessed on 21 July 2023). In

Ibiza and Formentera, the increase was relatively higher, growing from 144,313 in. to 374,151 in. Similar figures were reported by other scholars for the year 2009 [6].

Several administrations rely on seawater desalination to ensure freshwater availability [7,8]. While advances have been made to render desalination energetically more efficient [9], this technology still produces a large volume of byproducts and consumes a large amount of energy, therefore exerting a negative socio-environmental impact (e.g., greenhouse emission, brines accumulation, water taxes).

Rainwater harvesting is widely acknowledged as a simple, inexpensive and sustainable worldwide solution to fight the freshwater crisis [10–12]. It is among the oldest solutions to save water in dry regions [13] and after decades of abandonment, it is regaining momentum among researchers [14–18]. Rainwater harvesting refers to the collection of rainwater during periods of abundance (wet periods), to be reused later, when water is scarce (dry periods). Rainwater harvesting has been historically performed in Spain (for instance, through the so-called *aljibes*, a Spanish term that refers to underground water tanks). After years of abandonment, these solutions have been recovered by the administration. In the Balearic Islands, *aljibe*-like storage systems are now mandatory for all new private buildings [19]. The collection and storage of rooftop rainwater is possibly the most popular harvesting technique [18,20,21], but the limited areal surface of private houses' rooftops is typically not sufficient to generate sufficient volumes to balance out the water consumptions of these properties.
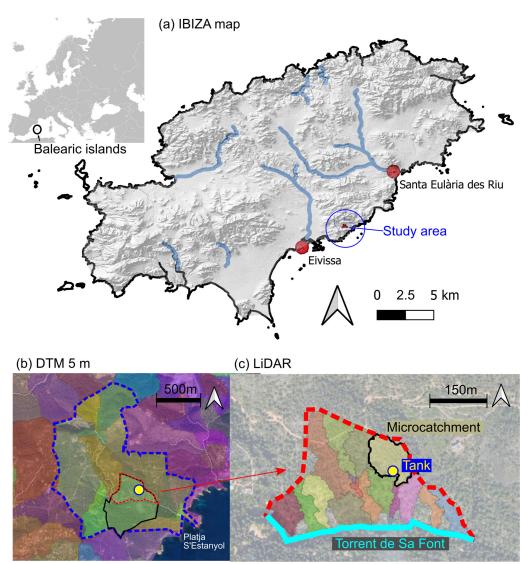
Ground-runoff harvesting (GRH) consists of collecting rainfall-generated runoff and storing it in tanks or using it directly, for instance for farming purposes. This method had a strategic historical importance for the development of ancient civilizations in dry areas, such as in the Negev desert in Israel [22]. Compared to rooftop rainwater harvesting, larger water volumes can be collected using GRH, particularly in hilly rural watersheds. Stormwater harvesting [23] is a form of GRH usually associated with the collection of urban runoff, which is polluted and requires treatment before being reused. When GRH is performed in natural areas, however, collected water may not need to be treated before being reused for non-drinking purposes, such as gardening and crop growing [24,25].

We contend that GWH should be promoted as a sustainable and inexpensive solution to increase freshwater availability in Mediterranean islands, such as Ibiza. In the central part of this hilly island, several private households remain disconnected from the main water distribution network. According to the Balearic Institute of Statistics, in 2021 some 27,700 people lived in isolated households of Ibiza, i.e., about 18% of the total island's population (152,820). Some of these households are villas with extensive land surfaces that include gardens and lawns requiring frequent irrigation. Water is usually obtained from private wells or delivered by trucks. The 2022 Hydrological Plan of the Balearic Islands indicates a total consumption of about 21% of the whole island's water demand by isolated households, but the actual number may be higher due to unregulated and illegal groundwater drafting or water distribution with trucks.

This paper describes the results of a study performed in 2022 that aimed to evaluate the potential of GWH in a hilly watershed located some 1.5 km off Platja de s'Estanyol in Ibiza (Figure 1a). A modular tank with about 40 m^3 of water storing capacity was constructed and buried in the shallow underground of a private estate. The tank was connected to a series of surface channels that intercepted runoff forming on a cultivated part of the terraced watershed and from the forest soil. The GWH had a double purpose of collecting water for watering the extended garden and crops of the estate while reducing stormwater downgradient of it, limiting soil loss and flooding risk.

The study was designed to quantify the accumulation rate of water in the tank during an extreme rainfall event. A model analysis was then developed to simulate runoff volumetric rates in the watershed using a widely known approach. An upscaling exercise was conducted to determine the potential of the approach to reduce water consumption at the scale of the island. By documenting this research, our broader aim was to create confidence

among stakeholders, governments, and administrations, hoping to convince them of the potential use of this simple green and inexpensive approach for freshwater saving.

Figure 1. (**a**) Hillshade map of Ibiza, showing the major surface water streams (blue lines) and position of the study area. (**b**) Catchment areas using the 5 m digital terrain model (DTM), which result in several watersheds subunits. Blue dotted line represents the extension of the watershed. (**c**) Extension (red dotted line) of the experimental 1.23 ha micro-catchment obtained from the Lidar analysis. Light blue line indicates the Torrent de Sa Font creek. The underground tank (yellow circle) is located in the closing section of the micro-catchment.
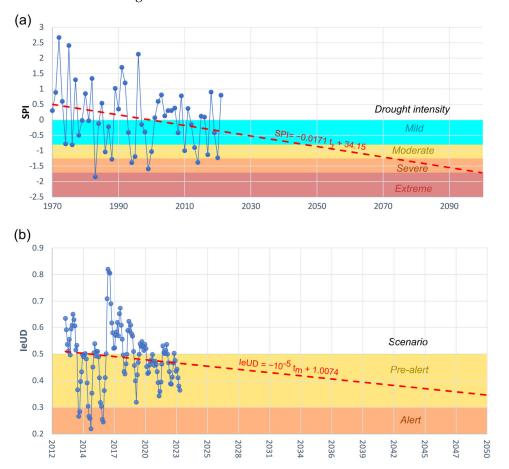
2. Materials and Methods

2.1. Geomorphology and Climate

The island of Ibiza is located in the Balearic archipelago, some 78 km off the east coast of Spain. It covers an area of 572 km^2, with a hilly configuration generating a variety of small-scale watersheds, as shown in Figure 1b,c (details about the methods adopted to generate these watersheds are provided in the following sections). The Balearic hydrological plan labels seven intermittent streams as rivers, although there are no permanent rivers on the island. Ibiza is characterized by a typical Mediterranean climate. Hot dry summers (June–September) are followed by a short period with intense storms (September–October). The remainder of the fall, winter and spring show low-intensity rainfalls.

Droughts are recurring in Ibiza, but in the last few years their frequency has been increasing. Figure 2a shows the evolution of the well-known Standardized Precipitation Index [26] calculated using average yearly precipitation data collected at the B954 "*Aeroport Eivissa*" (Ibiza airport) weather station (https://www.caib.es/sites/aigua/ca/index_de_sequera/; accessed on 12 December 2023). Raw data are available from the AEMET Open Data Website (Spain's State Meteorological Agency: *Agencia Estatal de Meteorologia* in Spanish). A negative SPI indicates a period of drought. The more negative the index, the more severe the drought.

Figure 2. (**a**) Evolution of the Standardized Precipitation Index (SPI) for the Ibiza Airport station (1970–2023). t_y = time unit (year) (**b**) Evolution of the drought status index for a unit of demand (IeUD) for Ibiza (2013–2023). t_m = time unit (month). Data from https://www.caib.es/sites/aigua/ca/index_de_sequera/ (accessed on 12 December 2023).

Out of the 52 years between 1970 and 2021 used for the calculation, 21 years were classified as moderate (SPI < −0.85) or as mild (SPI < −1.30). Three years were considered as severe (SPI < −1.35) and one (in 1983) as extreme (SPI < −1.65). Similar values were calculated using the Can Palerm station located in the town of Santa Eulalia. Notice that the best-fit linear model fitting the data (red line) shows a well-defined negative trend. Extrapolating the model leads to predicting moderate-to-severe drought conditions between 2050 and 2100.

A similar negative trend results from the analysis of another common drought index adopted in the Balearic Islands, called *Índex d'estat de sequera d'una unitat de demanda* (IeUD), translated as "drought status index of a unit of demand" (Decree 54/2017, BOIB [in Catalan and Spanish]) (Figure 2b). The IeUD is calculated for each unit of demand based on a weighted average of the drought status of a water mass located in a specific zone in the Balearic Islands, as mapped in the indicated decree. The whole island of Ibiza is considered as one single unit of demand. Details about the calculation of this

index can be found in article 10 of the decree. In short, this index is calculated on a monthly basis and represents a deviation of simple indicators referring to each type of water body (head levels of an aquifer; water lead in a lake or stream; discharge rate of a spring) from an historic trend. The more negative the IeUD, the more dangerous the drought. The index provides scenarios, or conditions, that enable the Government to take actions with different levels of severity to mitigate risks connected to potential lack of freshwater resources on the island. Available data were generated between June 2013 and June 2023 (https://www.caib.es/sites/aigua/ca/index_de_sequera/; accessed on 12 December 2023).

Data indicate that, in the last decade Ibiza has experienced months of "pre-alert" conditions ($0.50 > \text{IeUD} \geq 0.30$). In this scenario, mild measures are taken by the Government. These include increasing public awareness about the drought and actions that citizens can take to mitigate the problems (e.g., saving water at home) and preparing all the production lines of the desalination plants that can provide water to the units of demand that are in this situation. Each of these lines must gradually be put into operation until the maximum capacity of all desalination plants is reached, to achieve full performance in a potentially incoming scenario of alert or emergency. While no alert scenario has occurred in recent years, the negative trend determines an increase in the probability of alert or emergency conditions taking place in Ibiza in the future.
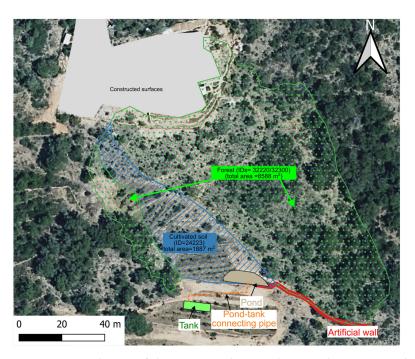
2.2. Water Tank Installation

In 2019, a modular water tank was built and installed in the private land of a villa (Figure 3). The tank was connected to a superficial pond with an estimated capacity of about 15 m^3. To avoid dust and organic material ending up in the tank, an additional curved sieve (auto-cleaning) filter of 200 micron was installed. Runoff flowing to the pond originates from the terraced and forest soils. When the pond is filled up, overflow water from the pond is diverted into the underground tank.
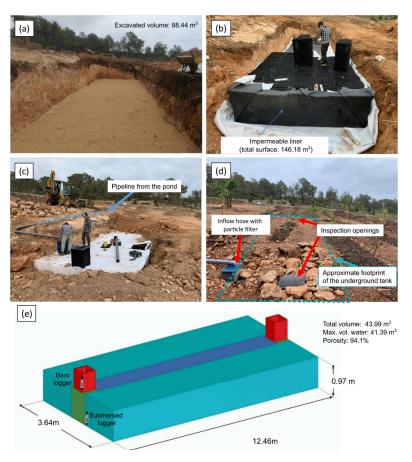
The tank was created and set up in three different steps, as graphically depicted in Figure 4. Initially, (a) some 90 m^3 of shallow soil were excavated up to a depth of about 1.5 m from the ground surface. (b) The tank was assembled inside the excavation site and covered with an impermeable (EPDM rubber) liner. The tank skeleton is a modular structure formed by a combination of multiple porous boxes, called "geocells" (Hydrostank S.L., Tafalla, Navarra, Spain). Some 130 geocells were needed to create a 12.46 m × 3.64 m × 0.97 m (x,y,z) tank, for a total volume of 43.81 m^3. The geocells were not filled in, leaving room for water to circulate across them, forming a porous skeleton. The tank achieved an effective porosity of 94.47%, being able to store a total water volume of 41.39 m^3 at its maximum capacity. The tank was connected to the pond through the external pipeline receiving runoff water (Figure 4c).

At the end of the construction, the ground surface of the buried tank appeared as in Figure 4d. Today, the surface is covered by plants (including edible fruit plants) and grassland. Figure 4e shows the conceptual scheme of the tank after its completion. There are two openings for inspection in the tank, located at the two extremes of the structure. The openings are empty geocells, which allow access to the bottom of the tank. On 18 June 2022, two submersible dataloggers for automatic measurement of water level at fixed time intervals (TD-Diver, Van Essen Instruments B.V., Delft, The Netherlands) were inserted into the tank through one of the two openings (Figure 4e). One datalogger was installed at the bottom of the tank to measure the variation in water levels as the tank was emptied (for garden irrigation) or filled in (by stormwater accumulation). The bottom of the tank was taken as the datum ($z_0 = 0$). The other datalogger was located at the top of the opening, in contact with the air, to measure barometric pressure. Measuring such variation was needed to compensate for the water pressure measured by the submerged database and to obtain a more accurate estimation of the water levels. The dataloggers' accuracy was 0.05%. The reading frequency was set up to fixed intervals of one hour.

Figure 3. Aerial view of the micro-catchment, showing the constructed surfaces of the private household (gray), the land generating runoff (classified in the two main land uses, "forest" and "cultivated soil"), artificial wall (red). The location of the pond, the tank and the connecting pipe is also shown.

Figure 4. The building process of the underground tank and geometry of it. (**a**) Excavation. (**b**) Construction of the modular tanks using the porous geocells. (**c**) Tank finalization and connection to

pipeline. (**d**) Ground surface of the buried tank after completion. (**e**) Conceptual scheme of tank, showing the two openings for inspection and the position of the two loggers (the shallow one for barometric pressure measurement; the submersed one for water pressure measurement).

A well-established modeling approach was adopted for the determination of runoff volumes from rainfall events, to be compared with the experimental data. The method was based on (1) the estimation of the catchment area that contributed to the runoff volumes collected by the tank, (2) the estimation of the net precipitation contributing to runoff and (3) the amount of runoff volumes for the specific morphological conditions and land use.

2.3. Catchment Area Calculation

LiDAR ("Light Detection And Range") data obtained from a private drone flight were used to calculate the catchment size. The dataset was processed through the LiDAR data processing tool LAStools v.2.0.1, integrated in the open-source geographic information system platform QGIS v.3.16. As the number of LiDAR points in the experimental dataset (>22 million) exceeded the maximum number of points allowed in LAStool (5 million), we first obtained an estimation of the watershed area using 5 -m-resolution digital terrain models (DTMs) datasets PNOA 0789 and 0799, downloaded from https://centrodedescargas.cnig.es/ (accessed on 12 December 2023). The watershed calculation tool GRASS 7 v2.0, embedded in QGIS, was used for this purpose. Then, we clipped the LiDAR data to the extent of the DTM-estimated subbasin, reducing the dataset to 1,006,796 points, which was eventually used to define the micro-catchments in the watershed.

2.4. Estimation of Net Infiltration

Once the area of the micro-catchment contributing to GRH was computed, the next step was the estimation of the runoff volumes. For this purpose, we used the Curve Number (CN) method [27], possibly the most well-known approach to relate runoff volumes to a "net" precipitation (P_n), defined as $P_n = P - E - \Delta S$, where P is the total precipitation, E is evaporation and ΔS is the watershed storage. The CN method assumes that, when the watershed storage is filled, all net rainfall becomes runoff. The relationship between P_n and runoff volumes is purely empirical and based on tabulated CN values, which depend on the soil type and land use. Sediment, silt or muck accumulation are not included in the CN model.

The net precipitation P_n was computed as

$$P_n = \frac{(P - I_a)^2}{P + I_a + S} \tag{1}$$

where P [mm] is the total precipitation over a time interval and I_a [mm] is the initial abstraction, i.e., the initial precipitation threshold starting the runoff. The variable S is the potential maximum retention, i.e., a measure of the ability of a watershed to abstract and retain storm precipitation. Assuming that $I_a = 0.2S$, simple manipulation of Equation (1) leads to

$$P_n = \frac{(P - I_a)^2}{P + 4I_a} \tag{2}$$

For P, we used high-resolution precipitation measurements with a reading frequency of 5 min intervals recorded at the Can Esperanza—ISANTA 521 station (the closest private weather station at 1.5 km away, hosted by Weather Underground, WU).

For the estimation of I_a, we proceeded with two steps.

(Step 1) We obtained a general (i.e., "uncorrected") reference initial abstraction value (I_a') according to the 5.2-IC guidelines [28], a reference document in Spain for hydrological design in civil engineering applications. According to the 5.2-IC guidelines, the Pre-Betic geological system, to which Ibiza belongs, is dominated by "type-C" hydrological condi-

tions. In the studied area, there were three main soil types: two forest soils (ID = 32220 "Macaronesian heathland" and ID = 32300 "Sclerophilous vegetation") and a highly cultivated soil (ID = 24223, "Mosaic of annual crops with permanent irrigated land"). According to 5.2-IC tables, both forest soils have I'_a = 14 mm, while the cultivated soil has I'_a = 22 mm.

(Step 2) Since this table considers the mean soil moisture before precipitation, we applied a correction to consider the degree of moisture in the soil. Following the 5.2-IC guidelines, we computed the "corrected" initial abstraction I_a as

$$I_a = \beta I'_a \tag{3}$$

where β is the correction factor. Soil was considered as "Dry soil" when cumulative precipitation (P_{tot}) in the 5 days before a storm was $P_{tot} < 13$ mm for dormant plants or $P_{tot} < 35$ mm for growing plants. Soil was considered as "Normal soil" when $13 < P_{tot} < 32$ mm for dormant plants or $35 < P_{tot} < 52$ mm for growing plants. Soil was considered as "Wet soil" when $P_{tot} > 32$ mm for dormant plants or $P_{tot} > 52$ mm for growing plants. The experimental period was characterized by an unusually dry period. In the five days before 25 September 2022 (the date at which a major storm event occurred that was recorded by the dataloggers), $P_{tot} = 12$ mm. As such we considered the soil as "dry" for our modeling purposes. For the studied area, this resulted in $\beta = 2.28$, such that the corrected values of the initial abstraction were therefore $I_a = 32$ mm for the forest soil (ID = 32220/32300) and $I_a = 50$ mm for the cultivated soil (ID = 24223).

Following the rational method, total runoff volumes (V) [m³] were computed as

$$V = \sum_{i=1}^{N} 10^3 P_n(i) A(i) \tag{4}$$

where N is the number of subunits with same soil type (N = 2 in this work) and A [m²] is the relative area of each portion of land with the same soil type. Runoff rates (Q, [m³/s]) were then calculated as

$$Q = \int_{t_i}^{t_f} V \, \mathrm{d}t \tag{5}$$

where t [s] is time and t_i and t_f define, respectively, the initial and final time of the observation.

A concentration time (t_c) was computed to evaluate the time needed for the runoff flow to reach the underground tank. Among the multiple existing formulations for t_c, we chose the Bransby-Williams method [29], which states that

$$t_c = 14.467 L A^{-0.1} S^{-0.2} \tag{6}$$
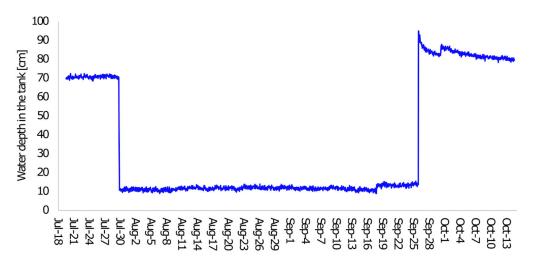
where t_c [min], L is the mainstream length [km], S is the mean catchment slope [-] and A is the catchment area [km²]. Other formulations, such as those included in the 5.2-IC norm and in Australian Rainfall and Runoff (ARR) guidelines, were tested, providing qualitatively similar results. The mean slope S was calculated using the maximum and minimum elevation of the micro-catchment obtained from the 5 m resolution DTM dataset (LiDAR data were deemed too sensitive to anthropogenic or vegetated elements for this purpose).

3. Results

3.1. Experimental Data

Figure 5 shows the evolution of the water levels in the tank recorded by the submerged datalogger. The plotted data are compensated for by the atmospheric pressure measured by the barometric datalogger. Raw data from both dataloggers have been uploaded to a public web repository (link in the Data Availability Statement section).

Figure 5. Water depth in the tank [cm] obtained after transforming water pressure in head levels (datum: base of the tank). The values are compensated for by the atmospheric pressure.

We found that the average initial water depth in the tank was about 0.70 m. This value, verified through manual measurements, corresponded to 72.1% of the tank elevation and was equivalent to a stored water volume of 29.8 m^3. Such existing water was collected through previous unmonitored runoff events. A sudden drop in the water levels was recorded on 29 June 2022, when the water was extracted by means of an electrical pump for watering the garden and small crops in the area. The tank was emptied almost entirely in about three hours, leaving some 0.13 m of water at the bottom of the reservoir. This corresponded to an unused water volume of about 5.55 m^3. The calculated average pumping rate was about 2.24×10^{-3} m^3/s, which is consistent with the type of pumps adopted in the zone. These initial observations served as a verification that the datalogger was properly functioning for the desired purposes. Water levels remained steady until 25 September 2022. This period corresponds to a persistent drought period in Ibiza, with a total cumulative rainfall < 100 mm and lack for significant storm events able to generate runoff.
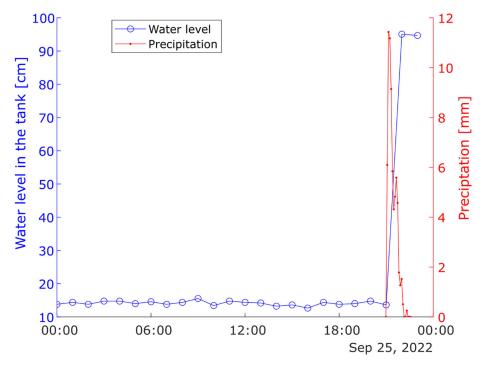
On 25 September 2022, a major storm hit the island, including the experimental site. Between 20:59 and 21:59, a cumulative rainfall depth ($\sum P$) equal to $\sum P = 67.6$ mm was measured at the Can Esperanza—ISANTA 521 station, as shown in Table 1. Another 0.8 mm was collected in the following 20 min and no more rainfall was collected in the following hours. The total cumulative rainfall for 25 September was 68.3 mm. Figure 6 compares the water levels measured on 25 September 2022 with the precipitation occurring on the same day. Between 9:00 pm and 10:00 pm, the water level increased from about 13 cm at 21:00 to 0.95 m at 22:00. This corresponds to an increase in volumetric capacity from 5.15 m^3 to 40.6 m^3, or from 13% to 98% in terms of relative tank capacity. Thus, the experiment demonstrated that the "harvesting rate" (H_R) of the tank was equal to $H_R = 35.45$ m^3/h. Notice that the rate could have been even higher than this, as the fixed reading intervals (1 h) of the datalogger did not allow evaluating if water levels reached 0.95 m in less time.

After 25 September 2022, water levels displayed a slow but constant decrease (Figure 7). The quasi-monotonic trend was interrupted by a few rainfall events, having, however, a minor impact on the tank capacity compared to the impact of the 25 September event. No gardening activities nor artificial water extraction were undertaken between 25 September 2022 and the end of the experimental time (15 October 2022). Evaporation is one reason for this loss, as the tank is not perfectly sealed. Root growth is another reason. Roots grew inside the geocells, as visually observed in the top part of the tank. Roots may have locally altered the impervious capacity of the geotextile, such that the tank started to empty out.
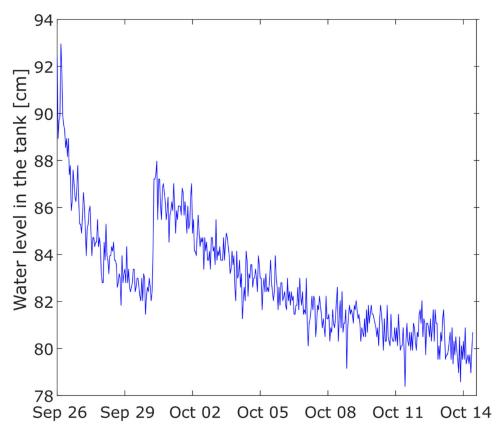
Table 1. Measured precipitation (*P* [mm]) at the Can Esperanza—ISANTA 521 station on 25 September 2022, and net precipitation (P_n [mm]) and ratio $\sum P_n{:}\sum P$ (as percentage) for the cultivated and forest areas.

	Total Precipitation		Cultivated Soil			Forest Soil		
time	P	$\sum P$	P_n	$\sum P_n$	$\sum P_n{:}\sum P$	P_n	$\sum P_n$	$\sum P_n{:}\sum P$
20:59	0.0	0.0	0.0	0.0		0.0	0.0	
21:04	6.1	6.1	0.0	0.0	0.0	0.0	0.0	0.0
21:09	11.4	17.5	0.0	0.0	0.0	0.0	0.0	0.0
21:14	11.2	28.7	0.0	0.0	0.0	0.0	0.0	0.0
21:19	9.1	37.8	0.0	0.0	0.0	0.2	0.2	0.6
21:24	5.8	43.7	0.0	0.0	0.0	0.6	0.8	1.8
21:29	4.3	48.0	0.0	0.0	0.0	0.7	1.5	3.0
21:34	4.8	52.8	0.0	0.0	0.0	0.9	2.4	4.5
21:39	5.6	58.4	0.2	0.3	0.5	1.3	3.7	6.4
21:44	4.6	63.0	0.4	0.6	1.0	1.3	5.0	8.0
21:49	1.8	64.8	0.2	0.8	1.2	0.5	5.6	8.6
21:54	1.3	66.0	0.1	1.0	1.5	0.4	6.0	9.0
21:59	1.5	67.6	0.2	1.2	1.8	0.5	6.5	9.6
22:04	0.5	68.1	0.1	1.2	1.8	0.2	6.6	9.8
22:09	0.0	68.1	0.0	1.2	1.8	0.0	6.6	9.8
22:14	0.0	68.1	0.0	1.2	1.8	0.0	6.6	9.8
22:19	0.3	68.3	0.1	1.3	1.9	0.1	6.7	9.8

Figure 6. Measured water depth in the tank and 5 min resolution precipitation on 25 September 2022. Markers indicate the time of the measurements (hourly for water level, every 5 min for precipitation).

Figure 7. Slow decline in water levels observed in the tank after the major storm on 25 September 2022. The monotonicity of the decreasing trend is interrupted by occasional rainfall events.

3.2. Model Based Interpretation

3.2.1. Catchment Area Calculation

The watershed delineated through the 5 m-resolution DTM is reported in Figure 1b. The watershed has an extension of about 2.05×10^6 m^2 and corresponds to one catchment area of the multi-branch Torrent de Sa Font creek, adjacent to the zone studied. Within this catchment zone, we identified several sub-catchments, among which the one corresponding to the studied zone (marked by a black line). This sub-catchment is divided into two halves, one to the north and one to the south of the creek. The experimental tank (yellow circle) falls within the north half (marked by a red dotted line). This area corresponds to the extension of LiDAR points used to refine the micro-catchment calculations.

Figure 1c shows the resulting micro-catchments calculated by the LiDAR analysis. The tank was located in the proximity of the closing section of a micro-catchment marked with black line. Figure 3 shows an aerial picture of the micro-catchment, overlaid by polygons delineating the distribution of soil types in the area. The micro-catchment includes constructed zones that do not contribute to the runoff calculation are grayed out, cultivated zones covering an area of about 1887 m^2 and forest zones covering an area of about 7588 m^2. In the bottom-right part of Figure 3, a red line highlights the presence of an artificial wall, not detected by the LiDAR data. Although this wall extended beyond the boundary of the micro-catchment calculated through GIS analysis, we believe that the wall could still contribute to funneling water towards the tank during heavy rainfall events. Thus, we incorporated an additional forest soil upgradient from the wall into the micro-catchment; the estimated extra area was 1000 m^2. Constructed surfaces forming the house footprint (gray areas in Figure 3) were not considered within the runoff calculation, as there are rainwater intercepting systems that prevent stormwater from accumulating around the house facility during heavy rainfall events. The estimated extension of such surfaces was 1812 m^2.

The resulting total areal extension of the micro-catchment that was assumed to contribute to GWR was, then, $A = 12{,}287$ m^2.

3.2.2. Runoff Calculation

We calculated the runoff rates (Q) generated during the storm event occurring on 25 September 2022 between 20:59 and 22:19 ($\Delta t = 1.33$ h). The total and net precipitation for the cultivated and forest areas inside the micro-catchment are reported in Table 1. The cumulative net precipitation ($\sum P_n$) calculated in the same Δt for the cultivated areas was $\sum P_n = 1.25$ mm, equivalent to 1.9% of $\sum P$. Runoff volumes produced in the cultivated areas were estimated as $V_C = 2.36$ m^3, such that $Q_C = 1.78$ m^3/h. For the forest areas, $\sum P_n = 6.72$ mm, equivalent to 9.8% of $\sum P$. Runoff volumes produced in the forest areas were estimated as $V_F = 57.72$ m^3, corresponding to a runoff rate of $Q_F = 43.40$ m^3/h. The cumulative volume is $V = V_C + V_F = 60.08$ m^3, corresponding a total runoff of $Q = 45.18$ m^3/h.

Recalling that runoff water was first conveyed to a collection pond with volume of 15 m^3, which was empty before starting the experiment, the runoff volumes entering the underground tank could be calculated as $V = 60.08 - 15 = 45.08$ m^3, corresponding to $H_R = 33.89$ m^3/h. This result is close to that obtained from the analysis of the water level in the tank ($H_R = 35.45$ m^3/h). Therefore, we consider that the experimental data validated the model result.

Using the Bransby-Williams equation, we found $t_c = 240.6$ s, which suggests that the runoff forming all over the site after the storm event happening in the evening of 25 September 2022 could have enough time to be collected by the tank in one hour. This value was obtained by assuming that $L = 132$ m (i.e., the full longitudinal extension of the micro-catchment). The DTM suggested a maximum elevation of 72 m and a minimum elevation of 43 m, separated by L. This results in $S = 0.22$, i.e., a moderately steep soil ("class 08") according to the FAO slope gradient classification [30].

4. Discussion
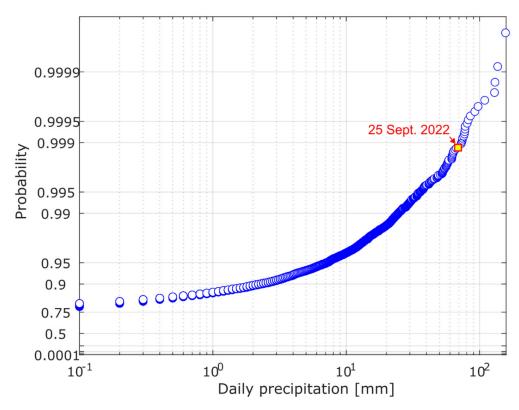
4.1. Probability of "Extreme" Events in Ibiza

The experimental results indicated that the underground system could store more than 35 m^3 of runoff water generated after an intense rainfall event of about 65 mm/h occurring on a micro-catchment of about 1.23 ha. The harvested volume of water corresponds to the volume of an average private swimming pool in Ibiza. Without the tank, this water would have been lost and an equivalent amount would have been obtained by conventional, less-sustainable water sources (e.g., groundwater) for gardening purposes.

It was not the first time that runoff water was harvested in the tank since its construction in 2019, according to visual inspections of the site, but we have no monitoring data prior to our experiment to establish a sound correlation between precipitation and runoff volumes. Thus, it is critical to evaluate if we merely monitored a "lucky", random event with low probability of return, or if similar runoff volumes can be expected multiple times each year.

To this end, we computed the probability plot of the daily precipitation measured at the Ibiza Airport station since 1970, the longest daily records available in Ibiza. Data were downloaded from the AEMET website. Available rainfall intensities at this station were equal to or above a minimum threshold of 0.1 mm/d. Unfortunately, in Ibiza, decade-long hourly rainfall measurements are lacking and a statistical analysis of sub-daily rainfall events cannot be computed. For instance, the Can Esperanza—ISANTA 521 station used for the rainfall–runoff model has been active since 2021.

The result, shown in Figure 8, indicates that the probability of occurrence (p) of daily precipitation events with an intensity $P < 0.1$ mm is $p = 75\%$ and with $P < 3$ mm is $p = 90\%$. Rare events exceeding $p = 95\%$ would correspond to precipitation depths of $P \geq 8$ mm/d. The rainfall event registered at the Can Esperanza station on the 25 September 2022 would correspond to $p = 0.0012$, i.e., an "extreme" event occurring once every 833 days.

Figure 8. Probability plot of the daily precipitation events [mm] measured at the Ibiza Airport station. The event measured during the study is marked in yellow on the graph.

Using the daily records measured at the Ibiza Airport, we computed the year-round average number of events by selecting a range of extreme rainfall intensities. For instance, the results, shown in Table 2, indicate that the number of events that occurred between $P = 20$ mm/d and $P = 30$ mm/d was $N_{ey} = 2.64$. In other terms, each year there is a chance of 2.64 events between $P = 20$ mm/d and $P = 30$ mm/d. The number of events that occurred between $P = 50$ mm/d and $P = 60$ mm/d is much lower and equal to $N_{ey} = 0.19$, as events with higher intensity become increasingly less frequent (i.e., more extreme).

Table 2. Precipitation range, equivalent precipitation (P_{eq} [mm/d]), average number of events per year for the precipitation range (N_{ey}) and expected annual runoff rates per year (Q_y [m^3/y]) using P_{eq}.

Precipitation Range	Equivalent Precipitation (P_{eq})	Number of Event per Year (N_{ey})	Expected Runoff Rates per Year (Q_y) Using P_{eq}
$\leq 20 < P < 30$	$P_{eq} = 25$	$N_{ey} = 2.64$	15.86
$\leq 30 < P < 40$	$P_{eq} = 35$	$N_{ey} = 1.01$	1.73
$\leq 40 < P < 50$	$P_{eq} = 45$	$N_{ey} = 0.38$	2.45
$\leq 50 < P < 60$	$P_{eq} = 55$	$N_{ey} = 0.38$	7.15
$\leq 60 < P < 70$	$P_{eq} = 65$	$N_{ey} = 0.19$	7.15
$\leq 70 < P < 80$	$P_{eq} = 75$	$N_{ey} = 0.21$	13.03
$\leq 80 < P < 90$	$P_{eq} = 85$	$N_{ey} = 0.06$	5.48
$\leq 90 < P < 100$	$P_{eq} = 95$	$N_{ey} = 0.04$	4.74
$P \geq 100$	$P_{eq} = 105$	$N_{ey} = 0.10$	15.37
Sum			72.95

We used N_{ey} to compute the expected runoff rate in the study site. Assuming that daily rainfall rates are equivalent to hourly rainfall rates (an assumption motivated by the lack of long hourly records to compute more accurate statistics), we first computed an equivalent precipitation (P_{eq}) as the mean precipitation for each precipitation interval. Then, we repeated the estimation of the runoff volumes for each precipitation range by inserting P_{eq} into Equation (2) and multiplying the resulting Q by N_{ey}. The results indicate that, while more frequent low-intensity precipitation events ($\leq 20 < P < 30$) can produce about Q = 15.86 m^3/year, more extreme events have a critical role in the GRH. Given their high rainfall intensity, just a handful of events can generate large runoff volumes that can be stored in the tank. For instance, while for the interval $\leq 60 < P < 70$, with P_{eq} = 65 mm/d the number of rainfall events is $N_{ey} = 0.19$ (i.e., less than one event every 5 years), the generated runoff is $Q \approx 7.15$ m^3/year, i.e., half of the produced by the more frequent less-extreme events.

The expected annual cumulative volume of water that can be collected in a single micro-catchment like the one studied is about V = 72.95 m^3. This means that, in the study site, about two tanks would be needed to harvest the expected amount of runoff generated in the catchment.

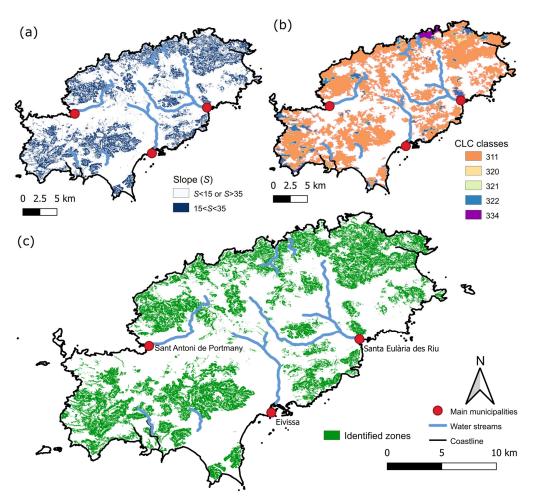### 4.2. Potential Impact of GRH at the Scale of the Island

All calculations presented so far were limited to the micro-catchment analyzed. It is, however, important to evaluate if the proposed solution can have a significant impact if adopted as an established rainwater harvesting method across the whole island. As a first-cut upscaling procedure, we proceeded as follows.

We first used QGIS to classify the zones of the island with similar soil slopes (S) to those found in the micro-catchment, where the average slope was S = 0.22. An estimation of the local gradient was performed using the 5 m-resolution DTM. Areas with a soil slope between S = 0.15 and S = 0.30 are shown in blue in Figure 9a. Then, we computed the area of the island classified as forest soils according to the well-known Corine Land Cover (CLC) 2018 dataset (https://land.copernicus.eu/pan-european/corine-land-cover/clc2018, accessed on 12 December 2023). For simplicity, we did not consider cultivated lands in this upscaling exercise. The resulting areas are shown in Figure 9b.
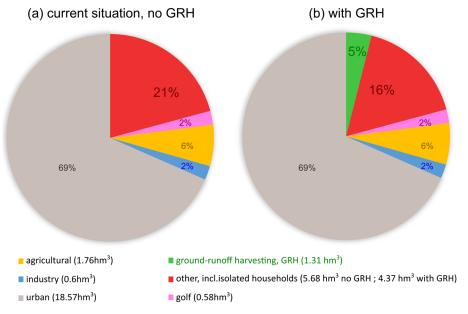
The areas of the island satisfying these criteria are shown in green in Figure 9c and correspond to $A = 1.58 \times 10^8$ m^2, which corresponds to an area $N_T \approx 18{,}300$ times the size of the studied micro-catchments. Rescaling the expected annual cumulative volume of water that can be collected in the analyzed micro-catchment (V = 72.95 m^3) by N_T leads to an estimated V = 1,317,600 m^3 could be saved using GRH in Ibiza. Such an amount corresponds to some 5% of the current water demand in Ibiza, according to the Hydrological Plan of the Balearic Islands, 2019. Figure 10 displays such water demand by activity and sector. Notice that this graph includes a general category ("other"), which embeds the water demand of all isolated households, and which comprises some 21% of the total water demand (about 5.68×10^6 m^3). The implementation of GRH may reduce this percentage to 16% (about 4.37×10^6 m^3).

The potential volume of freshwater that could be saved each year using GRH is therefore huge, considering that the proposed solution is sustainable and inexpensive. Figure 9c can be considered as a "suitability map" for GRH on the island, noticing, however, that the green areas in the map include natural areas (e.g., parks, woodland) with no households that can reuse the harvested water in their proximity. It is unlikely that all areas identified on the map will be equipped with a tank or similar structure as in the studied area. Therefore, the volume of 1.31 hm^3 calculated above should be interpreted as an estimate of the runoff volume that is "lost" every year from an island which is almost constantly in a pre-alert situation of drought, and where each droplet of water should be saved.

Figure 9. (**a**) In blue, areas of Ibiza with calculated slope (*S*, as a percentage) between *S* = 15 and *S* = 35. (**b**) Areas classified using the Corine Land Cover (CLC) 2018 classes that correspond to forest soil. (**c**) in green, areas with slope (*S*) between 15 and 35 overlapping the selected CLC classes.

Figure 10. (**a**) Current water demand by sectors on the island of Ibiza, according to the Hydrological Plan of the Balearic Islands, 2019. (**b**) Scenario with ground runoff harvesting (GRH) implemented in the island in all forest areas with similar slopes to the study site.

4.3. Future Research Development

Planned developments of this initial study include the following activities. First, we aim to replicate the study in other areas of the islands to evaluate local runoff dynamics in different land types and slopes. Once a sufficiently large database is built and experience is gained, we plan to develop a more sophisticated model and perform more accurate numerical analyses, which may embed climate change scenarios, future land use change and other variables. In this initial work, we intentionally selected the CN method as a simple, cost-effective and widely known approach that any other hydrologist can adopt and replicate. Being aware of the limitations of the CN model, a (semi-)distributed numerical model is expected to provide a more physically based estimation of runoff volumes and water balance. A suitable approach could be based, for instance, on the widely adopted SWAT ("Soil & Water Assessment Tool") model [31], which has been successfully applied for rainwater harvesting calculations [32].

Ultimately, we note that a more comprehensive model analysis may also support socio-economic cost estimations of the proposed GRH solution compared with alternative (conventional) freshwater production methods [8]. For instance, the model could serve as a basis to corroborate whether the potential disadvantages of GRH (e.g., the need for pumping water out of an underground tank or the intervention and earthworks in natural areas) can be effectively compensated by the (expected) limited socio-economic costs associated with this technology.

5. Conclusions

Floating populations in Mediterranean islands need much more water than it can be naturally provided by surface or groundwater reservoirs. Desalination is widely deployed to cope with water demand, but, despite technological advances, it remains a poorly sustainable approach in the long term. Among the alternative solutions that are currently being investigated, we tested ground-runoff harvesting (GRH), an inexpensive manner to capture surface runoff and store it in tanks for later reuse. In this work, we specifically evaluated if GRH is a valid technique to increase water availability in the hilly watersheds of Ibiza (Spain).

We found that a single extreme rainfall event with an intensity of 65 mm/h and a duration of one hour created a runoff volume of about 60 m^3 in a micro-catchment close to 12,300 m^2 in area. This runoff volume was sufficient to fill a pre-sedimentation pond of about 15 m^3 and a buried modular tank of about 40 m^3. Given the type of land use (cultivated and forest areas), this water could be reused for gardening the land of one of the several private isolated properties of the island, which are disconnected from the water network.

The observations were satisfactorily matched by a Curve-Number (CN)-based runoff-rainfall model, which was subsequently used for an upscaling exercise aimed at evaluating the potential of GRH at the scale of the island. Considering solely the average occurrence of extreme precipitation events, we calculated that some 1.31×10^6 m^3 of freshwater could be saved each year by harvesting runoff forming in the forested areas of Ibiza with slopes comprised between $S = 0.15$ and $S = 0.35$. Such a volume of water is equivalent to about 5% of the total freshwater demand of the island.

The overarching conclusion of this study is that GRH has an impressive potential to reduce freshwater demand from standard natural (groundwater) and unnatural (desalinization) sources. Local administrations should promote GRH as a natural approach to save water in dry Mediterranean islands. More water could be saved through GRH than through conventional rooftop rainwater harvesting. As climate change is expected to increase the frequency and intensity of hydroclimatic extremes, collecting runoff water could also provide secondary indirect benefits, such as reducing soil loss and flood-related risks downstream of the GRH structures.

References

1. Borg Galea, A.; Sadler, J.P.; Hannah, D.M.; Datry, T.; Dugdale, S.J. Mediterranean Intermittent Rivers and Ephemeral Streams: Challenges in Monitoring Complexity. *Ecohydrology* **2019**, *12*, e2149. [CrossRef]
2. Calaforra, J.; Ballarin, L.; Gines, J.; Perleros, V.; Tiniakos, L. The Main Coastal Karstic Aquifers of Southern Europe. *Cost Action* **2004**, *621*, 85–95.
3. Bakalowicz, M. Coastal Karst Groundwater in the Mediterranean: A Resource to Be Preferably Exploited Onshore, Not from Karst Submarine Springs. *Geosciences* **2018**, *8*, 258. [CrossRef]
4. Bouderbala, A. The Impact of Climate Change on Groundwater Resources in Coastal Aquifers: Case of the Alluvial Aquifer of Mitidja in Algeria. *Environ. Earth Sci.* **2019**, *78*, 698. [CrossRef]
5. Custodio, E. Salinity Problems in Mediterranean and Island Coastal Aquifers in Spain. *E3S Web Conf.* **2018**, *54*, 00005. [CrossRef]
6. Gelabert Ferrer, B.; Barón Períz, A.; Rodriguez Perea, A.; Marí Escandell, M.; Palerm Berrocal, J.C. Analysis of Water Management in the Island of Ibiza. 2015. Available online: https://ibizapreservation.org/wp-content/uploads/2018/03/ibiza_water_report_english.pdf (accessed on 2 November 2023).
7. Edlinger, R.; Zaplana Gomila, F. Ibiza Seawater RO—Special Design Features and Operating Data. *Desalination* **1996**, *105*, 125–134. [CrossRef]
8. Pérez, D.M.G.; Martín, J.M.M.; Martínez, J.M.G.; Sáez-Fernández, F.J. An Analysis of the Cost of Water Supply Linked to the Tourism Industry. An Application to the Case of the Island of Ibiza in Spain. *Water* **2020**, *12*, 2006. [CrossRef]
9. Kucera, J. (Ed.) *Desalination: Water from Water*, 2nd ed.; Wiley: New York, NY, USA; Scrivener Publishing LLC: Hoboken, NJ, USA; Salem, MA, USA, 2019; ISBN 978-1-119-40774-4.
10. Custódio, D.A.; Ghisi, E. Impact of Residential Rainwater Harvesting on Stormwater Runoff. *J. Environ. Manag.* **2023**, *326*, 116814. [CrossRef]
11. Raimondi, A.; Quinn, R.; Abhijith, G.R.; Becciu, G.; Ostfeld, A. Rainwater Harvesting and Treatment: State of the Art and Perspectives. *Water* **2023**, *15*, 1518. [CrossRef]
12. Palla, A.; Gnecco, I.; La Barbera, P. The Impact of Domestic Rainwater Harvesting Systems in Storm Water Runoff Mitigation at the Urban Block Scale. *J. Environ. Manag.* **2017**, *191*, 297–305. [CrossRef]
13. Amos, C.C.; Rahman, A.; Mwangi Gathenya, J. Economic Analysis and Feasibility of Rainwater Harvesting Systems in Urban and Peri-Urban Environments: A Review of the Global Situation with a Special Focus on Australia and Kenya. *Water* **2016**, *8*, 149. [CrossRef]
14. Odhiambo, K.O.; Iro Ong'or, B.T.; Kanda, E.K. Optimization of Rainwater Harvesting System Design for Smallholder Irrigation Farmers in Kenya: A Review. *J. Water Supply Res. Technol. Aqua* **2021**, *70*, 483–492. [CrossRef]
15. Kakoulas, D.A.; Golfinopoulos, S.K.; Koumparou, D.; Alexakis, D.E. The Effectiveness of Rainwater Harvesting Infrastructure in a Mediterranean Island. *Water* **2022**, *14*, 716. [CrossRef]
16. Liu, Y.; Li, G.; Zeng, P.; Zhang, X.; Tian, T.; Feng, H.; Che, Y. Challenge of Rainwater Harvesting in Shanghai, China: A Public Psychological Perspective. *J. Environ. Manag.* **2022**, *318*, 115584. [CrossRef] [PubMed]
17. Patil, D.; Kumar, G.; Kumar, A.; Gupta, R. A Systematic Basin-Wide Approach for Locating and Assessing Volumetric Potential of Rainwater Harvesting Sites in the Urban Area. *Environ. Sci. Pollut. Res.* **2022**, *30*, 14707–14721. [CrossRef] [PubMed]
18. Szabó, Z.; Pedretti, D.; Masetti, M.; Ridavits, T.; Csiszár, E.; Falus, G.; Palcsu, L.; Mádl-Szőnyi, J. Rooftop Rainwater Harvesting by a Shallow Well–Impacts and Potential from a Field Experiment in the Danube-Tisza Interfluve, Hungary. *Groundw. Sustain. Dev.* **2023**, *20*, 100884. [CrossRef]
19. GOIB. *Portal Del Agua de Las Islas Baleares-Pla Hidrológico (2022–2027)*; GOIB: Palma de Mallorca, Spain, 2023.
20. Campisano, A.; Butler, D.; Ward, S.; Burns, M.J.; Friedler, E.; DeBusk, K.; Fisher-Jeffes, L.N.; Ghisi, E.; Rahman, A.; Furumai, H.; et al. Urban Rainwater Harvesting Systems: Research, Implementation and Future Perspectives. *Water Res.* **2017**, *115*, 195–209. [CrossRef] [PubMed]

21. Bañas, K.; Robles, M.E.; Maniquiz-Redillas, M. Stormwater Harvesting from Roof Catchments: A Review of Design, Efficiency, and Sustainability. *Water* **2023**, *15*, 1774. [CrossRef]

22. UN Habitat. *Blue Drop Series on Rainwater Harvesting and Utilisation—Book 3: Project Managers and Implemetation Agency*; UN Habitat: Nairobi, Kenya, 2005.

23. Feng, W.; Liu, Y.; Gao, L. Stormwater Treatment for Reuse: Current Practice and Future Development—A Review. *J. Environ. Manag.* **2022**, *301*, 113830. [CrossRef]

24. Norfolk, O.; Abdel-Dayem, M.; Gilbert, F. Rainwater Harvesting and Arthropod Biodiversity within an Arid Agro-Ecosystem. *Agric. Ecosyst. Environ.* **2012**, *162*, 8–14. [CrossRef]

25. De Winnaar, G.; Jewitt, G. Ecohydrological Implications of Runoff Harvesting in the Headwaters of the Thukela River Basin, South Africa. *Phys. Chem. Earth Parts A/B/C* **2010**, *35*, 634–642. [CrossRef]

26. McKee, T.B.; Doesken, N.J.; Kleist, J. The Relationship of Drought Frequency and Duration to Time Scales. In Proceedings of the 8th Conference on Applied Climatology, Boston, MA, USA, 17–22 January 1993; Volume 17, pp. 179–183.

27. USDA-SCS. *National Engineering Handbook, Section 4: Hydrology*; USDA-SCS: Washington, DC, USA, 1972; p. 548.

28. Spanish Ministry of Development. *Norma 5.2–IC de la Instrucción de Carreteras. Drenaje Superficial. Dirección General de Carreteras, Ministerio de Fomento, Gobierno de España. BOE Del 5 de Junio de 2018*; Spanish Ministry of Development: Madrid, Spain, 2019. (In Spanish)

29. Bransby, W.G. Discussion on Flood Discharge from Catchment Areas. In *Minutes of Proceedings of the Institution of Civil Engineers*; Institution of Civil Engineers: London, UK, 1924; Volume CCXVII, pp. 421–424.

30. Jahn, R.; Blume, H.P.; Asio, V.B.; Spaargaren, O.; Schad, P. *Guidelines for Soil Description*, 4th ed.; FAO: Rome, Italy, 2006; ISBN 978-92-5-105521-2.

31. Arnold, J.G.; Srinivasan, R.; Muttiah, R.S.; Williams, J.R. Large Area Hydrologic Modeling and Assessment Part I: Model Development 1. *JAWRA J. Am. Water Resour. Assoc.* **1998**, *34*, 73–89. [CrossRef]

32. Luo, K.; Li, Y. Assessing Rainwater Harvesting Potential in a Humid and Semi-Humid Region Based on a Hydrological Model. *J. Hydrol. Reg. Stud.* **2021**, *37*, 100912. [CrossRef]